

**- RESEARCH ARTICLE -****GMT-based geological mapping and assessment of the bathymetric variations of the Kuril-Kamchatka Trench, Pacific Ocean**

Polina Lemenkova\*

Ocean University of China, College of Marine Geo-sciences, Qingdao, China.

**Abstract**

This manuscript summarizes the results of the geospatial analysis undertaken by means of Generic Mapping Tools (GMT). The comparative assessment of the bathymetry of the Kuril-Kamchatka hadal trench was performed for southern and northern segments separated by the Bussol Strait. The formation of the hadal trench is affected by the impacts of local geological and geophysical settings varying along the trench. The methodological approach is as follows. The profiling was undertaken using GMT modules 'grdimage', 'grdtrack' and 'psxy'. The modelling consists of the collected data of 10706 observation samples from 52 profiles in southern part and 12726 from 62 profiles in the northern segment. The GMT modules 'psrose' and 'pshistograms' were used to plot histograms and rose diagrams visualizing bathymetric variables of depths. The geology was mapped using GMT modules 'pscoast', 'grdcut', 'grdcontour' and 'psxy' to plot lineaments and geological objects (ophiolites, faults, earthquakes, trench, magnetic anomalies, tectonic slabs, fracture zones and volcanoes). The base map is based on the ETOPO Global Relief Model. The comparison of the bathymetry shown variations in the northern and southern segments: southern part reaches -8,200 m maximal depths while northern has -7,800 m. This is influenced by the geological settings: earthquakes magnitude and seismicity are higher in the south-west. The submarine terraces and floodplains were observed at -4000 m depth forming landforms located southwards off the Bussol Strait. This geospatial analysis contributes to the development of the geological mapping with an example of the Kamchatka area, a region with high seismicity and repeated earthquakes.

**Keywords:**

GMT, Bathymetry, Modelling, Mapping, Geospatial Analysis

**Article history:**

Received 26 July 2019, Accepted 29 January 2020, Available online 19 February 2020

---

\* Corresponding Author: Polina Lemenkova, E:mail: pauline.lemenkova@gmail.com

## **Introduction**

The geographic object of this study is the Kuril-Kamchatka Trench, located in the north-west Pacific Ocean (Figure 1). The specific distinction of this hadal trench is its clear division into two parts: northern and southern segments separated by the Bussol Strait. The geological settings of the study area is characterized by high seismicity, repeated earthquakes, and tectonic instability caused by plate subduction. Geological factors differ in northern and southern parts of the trench, which naturally affects its geomorphology. The comparisons on the northern and southern parts of the Kuril-Kamchatka Trench seafloor are not assessed within the published literature. Therefore, the novelty of this study is a contribution towards the regional analysis of the geospatial variation of the trench geomorphology in its southern and northern parts.

The study aim is comparative geomorphic analysis of deep-sea oceanic trench: Kuril-Kamchatka Trench located in the geologically complex region of the north-western part of the Pacific Ocean. Complex geophysical settings results in formation of the trench, high seismicity, repetitive earthquakes and volcanism and geodynamic instability visualized on the thematic maps of geological and tectonic settings as the most important causes of the ocean trench formation. Cartographic objective of the study is to visualize bathymetry, geological settings, earthquakes, volcanoes and seismicity, depict lineaments of the tectonic slabs, areas of large igneous provinces, geomorphology, tectonic and geological settings of the trench. Additional aim is to perform statistical analysis for comparative depths distribution and aspect of the slopes in the southern and northern part of the Kuril-Kamchatka Trench.

The objective of this research was to detect differences in the northern and southern parts of the Kuril-Kamchatka Trench through performed comparative geostatistical analysis using a sequence of the presented GMT modules. Technically, this research is intended to establish a framework of the GMT based geospatial modelling and mapping using multi-source data to obtain a better understanding of the submarine shape of the Kuril-Kamchatka Trench, and to raise awareness of this unique location.

The tectonic properties of the study area mutually affect both land and submarine geomorphology. Thus, as noted by Pflanz et al. (2013), the location of the KKT at the meeting place of active Kuril–Kamchatka and Aleutian arcs causes the coastline of the Kamchatka Peninsula to be affected by strong tectonic activities. Fracture zones have variable influence on the uplift of the Kamchatka Peninsula. The geomorphic consequence include raise of the multi-level, highly uplifted marine terraces displaced along the active tectonic faults. Furthermore, the tectonic movements cause the uplift of the coastal sediments (Pflanz et al., 2013).

## **Material and Methods**

The research methodology is completely based on the use of the Generic Mapping Tools (GMT) cartographic scripting toolset that was used to map Figures 1, 2, 3 and 4. The GMT is a highly effective professional tool designed for mapping and developed by Wessel in Smith (Wessel & Smith, 1998). Comparing to the traditional GIS software, the advantages of the GMT consists in its flexibility provided by scripting approaches rather than GUI, as well as open source free availability. A great advantage is a cartographic functionality of this tool set: a large variety of the visualization, plotting, modelling, as well as advanced cartographic modules: mapping projections, modelling, grid raster data processing (Wessel & Smith, 1991). Due to the advantages of the GMT

that consists in its functionality, a wide range of the cartographic projections and availability of the modules the GMT was selected as the best cartographic tools for geospatial analysis that was performed using available documentation (Wessel & Smith, 2018; Wessel et al., 2019). In contrast to the classic cartographic approaches having Graphical User Interface (GUI), e.g. ArcGIS based, in geodata visualization and mapping (Suetova et al., 2005; Klaučo et al., 2013; Gauger et al., 2007; Klaučo et al., 2017; Lemenkova, 2011; Kuhn et al., 2006), the GMT is notable for its scripting algorithms as a core conceptual methodology.

### ***Bathymetric mapping***

Bathymetric mapping (shown on Figure 1) and plotting profiles was performed using ETOPO1 bathymetric grid with 1 minute resolution using existing methodology (Lemenkova, 2019g; Lemenkova, 2019h). The map was visualized on the study area square using a sequence of the GMT modules. A 'grdcut' module was used for cutting area of interest from the global grid earth relief 01m.grd by selecting coordinates -R, following by 'grdimage' module for visualizing the grid itself. Examples of the previous research on the semi-automated digitizing of the cross-section profiles in Quantum GIS for further modelling using R language were considered for general research workflow (Lemenkova, 2018a; Lemenkova, 2018b). The key code snippets are provided below: First, selecting study area from the grid was done using 'grdcut' module: `grdcut earth_relief_01m.grd -R140/170/40/60 -Gkkt_relief.ncgmt` Second, the image was visualized using 'grdimage' GMT module: `grdimage kkt_relief.nc -Cmyocean.cpt -R140/170/40/60 -JM6i -P -I+a15+ne0.75 -Xc -K > $ps` Third, the key points for northern and southern segments were selected by the code: `gmt ptext -R -J -N -O -K -F+jTL+f18p,Times-Roman,yellow+jLB >> $ps << EOF 161.0 48.3 Kuril-Kamchatka 161.0 47.5 Trench EOF` Then the profiles were plotted using GMT 'grdtrack' module (example for the northern part): `gmt grdtrack trench2.txt -Gkkt_relief.nc -C400k/2k/10k+v -Sm+sstack2.txt > table2.txt` The profiles were plotted using code: `gmt psxy -R -J -W0.5p table2.txt -O -K >> $ps` The text annotations were added using following (here example of Deryugin Basin): `gmt ptext -R -J -N -O -K -F+jTL+f14p,Times-Roman,black+jLB+a-75 -Gwhite -Wthinnest >> $ps << EOF 145.0 54.5 Deryugin Basin EOF`

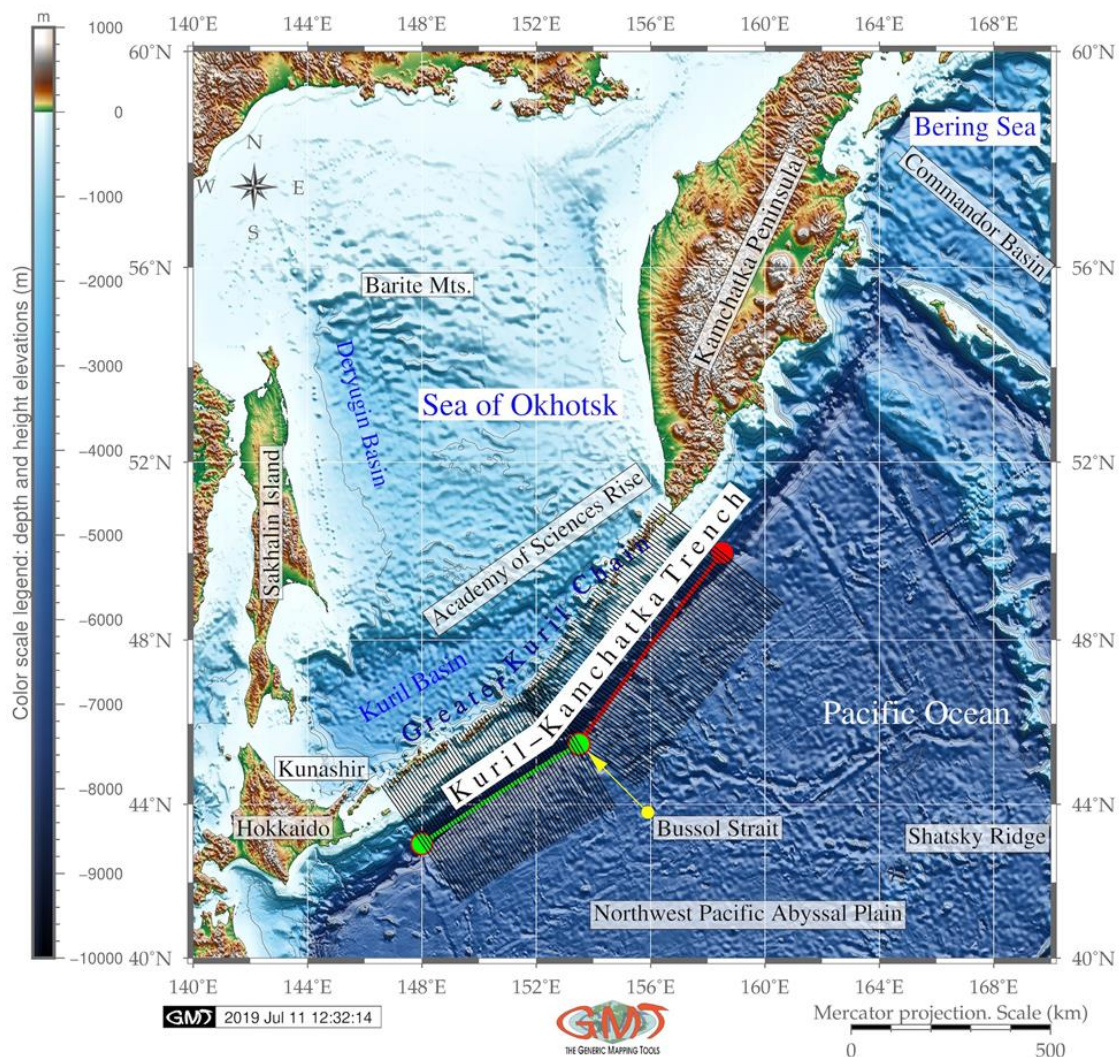


Figure 1. Study area: bathymetric map of the Sea of Okhotsk and Kuril-Kamchatka Trench.

### Geological mapping

The geological mapping (Figure 2) is based on the use of the sequence of the GMT modules. Several auxiliary modules were then used both for cartographic purposes (color scale, scale bar, directional rose, grid ticks and lines, etc) and for the map embellishment (GMT logo) using available techniques (Smith & Sandwell, 1997). The shoreline vector layers were driven from the existing GMT data sets (Wessel & Smith, 1996): tectonics, bathymetry, geomorphology and geology. The most important code are the following: The relief map from ETOPO5 was cut off using following code: `gmt grdcut earth_relief_05m.grd -R140/170/40/60 -Gkkt_relief.nc -V` Then the coastlines were added: `gmt pscoast -R140/170/40/60 -JL155/50/45/55/6i -P -W0.1p -Gpapayawhip -Slightcyan -Df -K > $ps` Bathymetric contours were added using the following GMT code by 'grdcontour' module: `gmt grdcontour @kkt_relief.nc -R -J -C500 -A2000+f9p,Times-Roman -S4 -T+d15p/3p -W0.1p -O -K >> $ps` Next step included plotting a sequence of the geological lineaments and objects:



- `gmt makecpt -Crainbow -T0/700/50 -Z > rain.cpt`
- `gmt psxy -R -J trench.gmt -Sf1.5c/0.2c+l+t -Wthick,red -Gred -O -K >> $ps`
- `gmt psxy -R -J ridge.gmt -Sf0.5c/0.15c+l+t -Wthin,darkcyan -Gpurple -O -K >> $ps`
- `gmt psxy -R -J LIPS.2011.gmt -L -Gpink1@50 -Wthinnest,red -O -K >> $ps`
- `gmt psxy -R -J ophiolites.gmt -Sc0.1c -Gmagenta -Wthinnest -O -K >> $ps`
- `gmt psxy -R -J volcanoes.gmt -Sc0.1c -Gpurple -Wthinnest -O -K >> $ps`

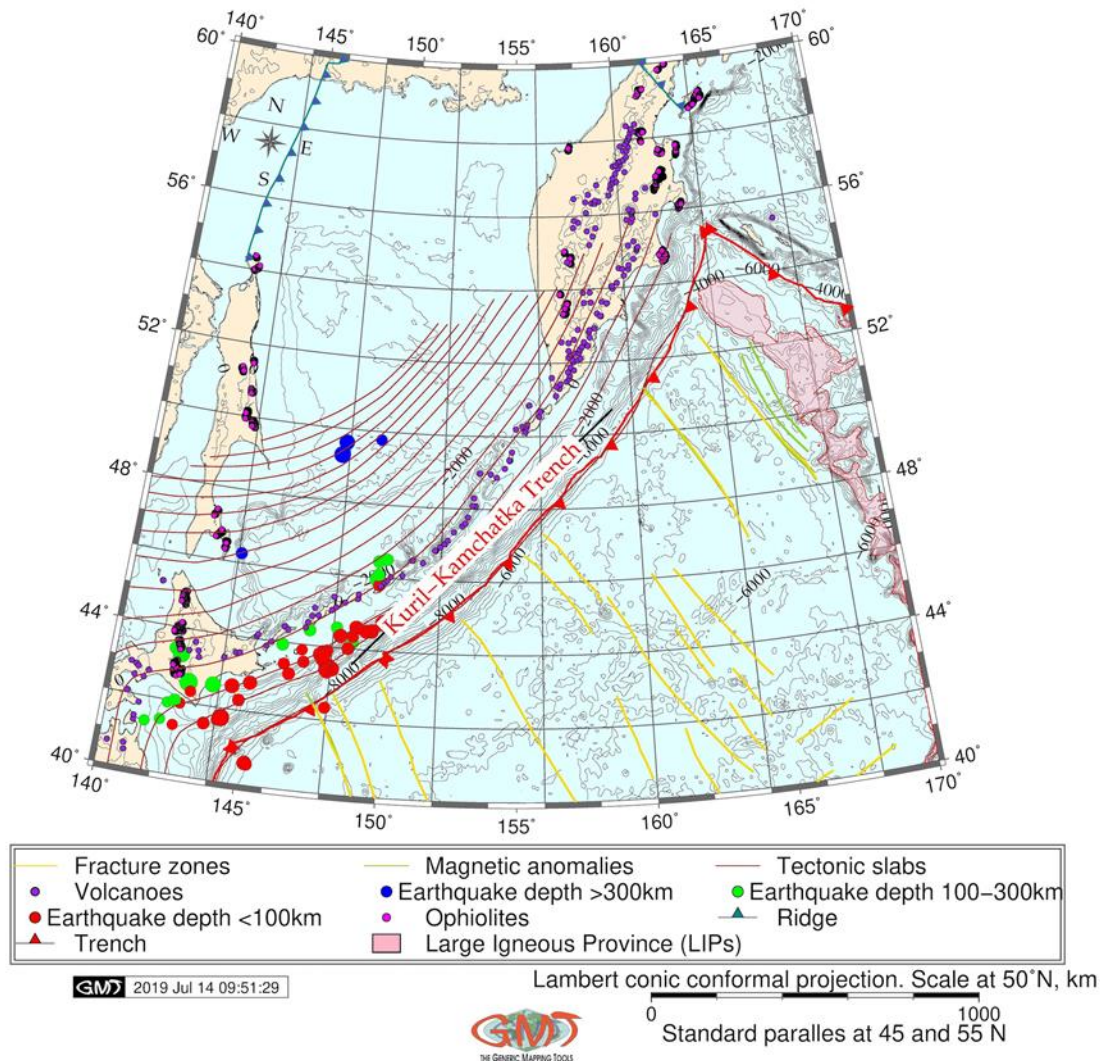


Figure 2. Geological settings of the study area: seismisity and earthquakes, geological lineaments and tectonic slabs in the Sea of Okhotsk and Kuril-Kamchatka Trench.

Example of the geological mapping of the hadal trench using Quantum GIS with a case study of the Mariana Trench, the deepest trench on the *Earth* (Lemenkova, 2019a) includes application of R programming, various statistical approaches towards data modelling (Lemenkova, 2019i; Lemenkova, 2019j), automatization in hydrographic data processing (Schenke &

Lemenkova, 2008). The scope of the research is more focused on the geological assessment than statistical analysis. Therefore, the special attention was paid to mapping geological lineaments, faults, trench extent, location of the Large Igneous Provinces, volcanic spots and earthquakes in the Kuril-Kamchatka Trench (Figure 2). Various depth of the earthquakes are presented in different colors, as well as fracture zones, ophiolites, magnetic anomalies and extension of the tectonic slabs (Figure 2).

### *Statistical 3D histograms*

Plotting statistical 3D histograms (shown on Figure 3) was performed using following sequence of the GMT codes: First, the available grid (file kkt\_bathy.nc) was uploaded to the GMT and converted to the xyz format: `gmt grd2xyz kkt_bathy.nc > kkt_bathy.xyz`

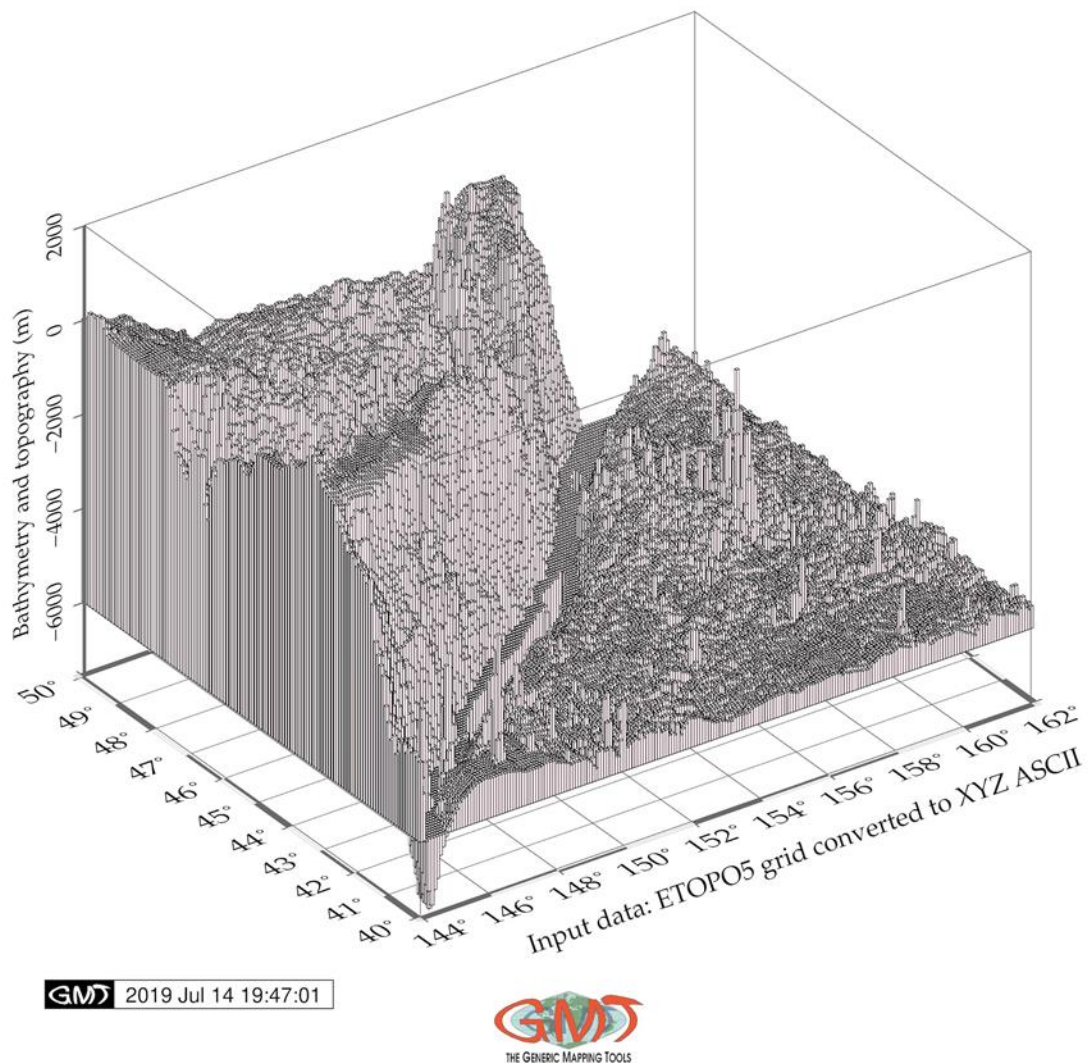


Figure 3. Statistical 3D histograms showing depths distribution in the southern part of the Sea of Okhotsk and Kuril-Kamchatka Trench.

Second, the file was checked up to define the depth/heights range: `gmt info kkt_bathy.xyz` Third, the 3D histogram from the data table was plotted using following code: `gmt psxyz kkt_bathy.xyz -Bpxa4 -Bpya2 -Bsxg2a2 -Bsyg1a1 -Bz2000+l"Bathymetry and topography (m)" -BWSneZ+b+t"3D-histograms of the depth values: Kuril-Kamchatka Trench" -R144/162/40/50/-7600/2000 -JM10c -JZ7c -p215/30 -So0.083ub-6000 -P -Wthinest -Glavenderblush -UBL/-15p/-35p -K > $ps`

### Statistical 2D histograms

Statistical histograms of data distribution were plotted using a sequence of the GMT modules: `gmtset`, `psrose`, `pshistogram`, `pslegend`, `logo` and `psconvert`. The histograms plots demonstrated frequency of the data distribution against bathymetric variables. The statistical techniques of the data analysis are widely used in geospatial studies, applied and described in previous works.

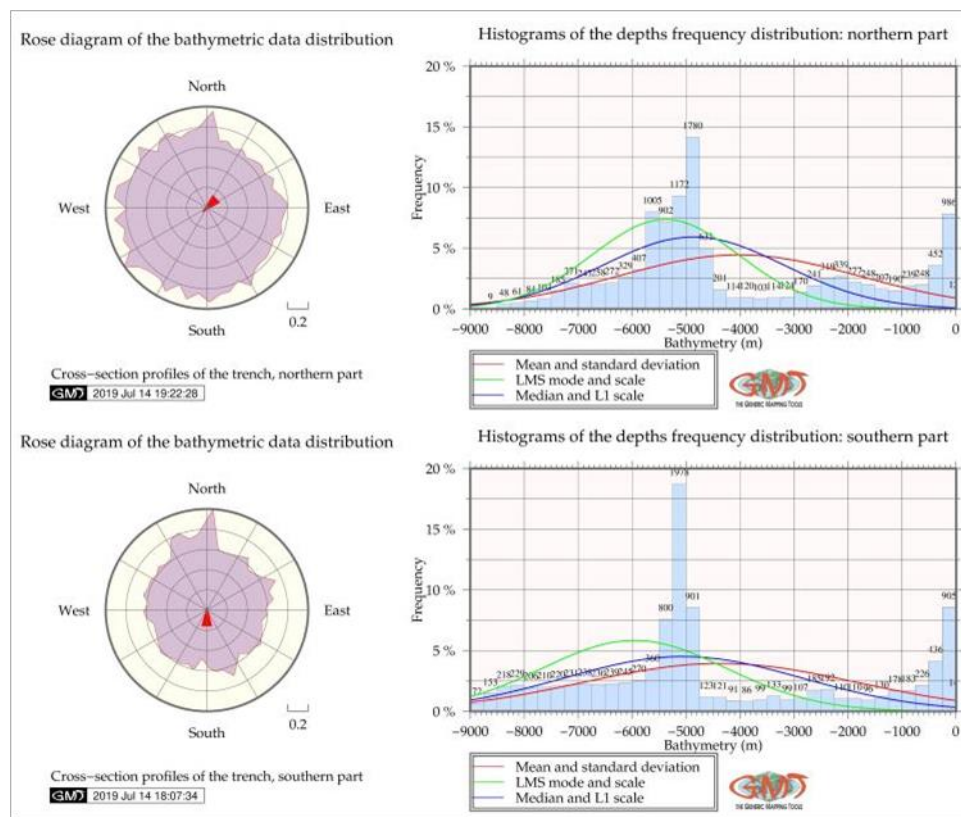


Figure 4. Statistical 2D histograms and rose diagrams showing comparative depths distribution in the southern and northern part of the Kuril-Kamchatka Trench. Rose diagram shows the aspect of the slopes.

Plotting statistical 2D histograms and rose diagrams (Figure 4) was done using following GMT code:

- `gmt psrose table2.txt -i1,4 -R0/1/0/360 -A7r -S1.0in -Gthistle -Bx0.2g0.2 -By30g30+l"Cross-section profiles of the trench, northern part" -B+t"Rose diagram of the bathymetric data distribution"+givory1 -M0.5c+e+gred+n1c -W0.1p,red -Cm -UBL/-1.4c/-2.3c -Vv -K > $ps`

- `gmt pshistogram table2.txt -i4 -R-9000/6/0/20 -JX4.8i/2.4i -X3.6i -Bpxg1000a1000f100+l"Bathymetry (m)" -Bpyg5a5f2.5+l"Frequency"+u" %" -Bsyg2.5 -BWSne+t"Histograms of the depths frequency distribution: northern part"+gsnow1 -Glightsteelblue1 -D+f7p,Times-Roman,black -L0.1p,dimgray -Z1 -W250 -N0+pred -N1+pblue -N2+pgreen -O -K >> $ps`

Statistical analysis of the geospatial data using histograms, Kernel Density Estimation Plots, boxplots, regression analysis and other types of statistical approaches and algorithms has been performed in previous research using Python programming with a case study of the Mariana Trench (Lemenkova, 2019b; Lemenkova, 2019c). Other examples demonstrate using IBM SPSS Statistics (Lemenkova, 2019e), statistical landscape metrics (Klaučo *et al.*, 2014) and Gretl software (Lemenkova, 2019d), AWK or Octave (Lemenkova, 2019f). However, the particular feature of this research consists in using GMT both for cartographic visualization and mapping, and for statistical plotting by modules 'psrose' and 'pshistogram'.

## Results

### *Southern segment of the Kuril-Kamchatka Trench*

The summary interpretation of the 52 NE–SW cross-section profiles across the KKT in the southern part (highlighted as green line on the Figure 1) shows following results. At the southern region (located in the proximity of the active volcanic spots, see Figure 2), the seafloor depths are found to decrease with increasing latitude gradually while moving northwards. Trench morphology in the northern termination of the southern segment of the KKT, just approaching the Bussol Strait is at the U-trending seafloor rise. Besides, there is indication of the slab subduction along the NW margin of the trench facing the Sea of Okhotsk. Here the trench-parallel, linear system of the southern part of the Greater Kuril Chain Islands (Iturup, Urup, Shikotan and minor chain of islands) provides a natural barrier to the extensive downslope sediment transport from the southern Okhotsk Sea to the trench. To a certain extent, they are trapped behind the chain of islands and further restrict the supply of the sediments to the central part of the trench downslope.

The submarine terraces are presented along the southern part of the trench axis. A common trend is that southern part of the seafloor depths are found to vary considerably, even within neighboring selected profiles. The wedge-shaped body of the trench is being developed in its southern part on the westwards trench slope in front of the Sea of Okhotsk inner trench wall closer to the islands Kunashir, Urup and Iturup from the Kuril Greater Chain. It shows a typical and distinct morphologic impact from the nearby subduction zone. The areas of the submarine terraces interspersed with the floodplains have been observed in the southern part of the trench at -4000 m depth forming distinctive patterns on the landforms located immediately southwards the Bussol Strait. The southern part of the KKT near Kuril Basin (Figure 1) creates conditions for the short sediment transport from the islands between the terrestrial sediments of the Sakhalin Island and the Kurils with marine sediments sinking to the trench. In the southern segment, the sedimentation system goes in a transverse direction of the trench stretching: it brings the sediments from the islands located on the south of Okhotsk Sea: Hokkaido, Kunashir, Iturup, Urup and minor islands of the southern part of Greater Kuril Chain. The southern part of the trench here serves as a sink for the sediment dispersal systems along the active margins of the Kuril Islands. Therefore, it is longitudinally fed by the sediments derived from the southern Kuril. Besides, the location of the



compression-extension tectonic slabs as demonstrated on the Figure 2 and the average deformation of the trench's axis is directly affected by the source of earthquakes located in the south of the Greater Kuril Chain.

### ***Northern segment of the Kuril-Kamchatka Trench***

The northern part of the KKT (highlighted as red line segment on the Figure 1) reflects in its morphological features the combined effects of tectonic slab subduction, collision, and sedimentation processes and closeness of the large igneous provinces (LIPs) in the northern part of the Pacific Ocean close to the Bering Sea. In particular they are being determined by the rate of the Pacific tectonic plate convergence, sediment supply, and the topography of the subducting seafloor. Fracture zones oriented in NW direction from the Pacific Plate towards the trench affect the sediment deposition in trench. Namely, the sediment deposits filling the trench are mostly controlled by the rate of the Pacific plate convergence towards Okhotsk tectonic plate. The analysis and interpretation of the 62 NE–SW cross-section profiles across the KKT in the northern part shows following results.

The sequence of profiles crossing the northern part of the trench show truncated landforms at the canyon walls of the Greater Kuril Chain, which rise ca. 1000 m a.s.l while southern part of the islands chain (Iturup and Urup islands) show ca. 400 m a.s.l. Processed numerical modelling based on the bathymetric ETOPO1 data from the area around the northern part of the trench identified features of the trench geomorphological system (submarine canyons, trench wedge, submarine ridges, and basins) in the northern part of the trench. The trench-parallel longitudinal sedimentation system carries sediments eroded from the Kamchatka orogenic system to the east, along the Kamchatka Peninsula. These deposits are then moved to the north-eastern part of the trench, shown as red line on Figure 1.

The northern part of the KKT receives the sediments transported in a southwest direction from the downslopes of the Kamchatka and northern islands. Trench-fill sediments are then mostly derived from the volcanic arcs formed by the Kamchatka and northern segment of the Kuril islands, as well as adjacent volcanic basins. From the Kurils the sediments are transported to the northern part of the trench bottom through the set of submarine canyons directed transverse to the axis of the northern KKT filling it by terrigenous sediments.

Orthogonal profiles line Nr. 1 and 7, located north of the KKT in perpendicular direction off the Academy of Sciences Rise (Figure 1) reveal the steeper shape form caused by the seismic characteristics and sedimentary accumulation patterns of the south-east parts of Sea of Okhotsk. The increased number of profiles while moving in northwards direction show shallower depths which illustrates previous discussion on the variations in the sedimentation processes of northern and southern part of the trench, and the landform of the profiles in the respective segments.

Farther down the trench and north-east of the Shiashkotan Island from the Kurils, profile line 42 and 49 cross take the form of an irregularly shaped trough of ca. 8 km width. The trench floor morphology here is characterized by the gentle slope patterns and depths not exceeding 7,400 m. On both profiles, the northern wall of the trench is the island-ward sloping surface of the Kuril islands. Profile line 56 shows mainly flat and parallel form at the shallower depths that extend to about 7,200 m in the seafloor. Further profile line 62 shows even more shallower depth and gentle slope shape following the enlargement of the trench valley starting northwards from the Paramushir

Island. Stacks of local small hills and bulges across the trench indicate multiple sediment deposition processes along the trench slope in its northern part.

## Discussion

### *Comparison of the southern and northern segments*

Comparing northern and southern parts of the trench, the wedge-like or U-shaped morphology of the trench in two parts south- and northwards from the Bussol Strait are distinct not only from the inner-ward slope facing the Sea of Okhotsk and the Greater Kurils Chain, but also in longitudinal direction along the trench axis. This particular may be explained by the response to the gradual changes in seafloor topography patterns. Another impact can be added by the oceanological factors, such as intensive bottom currents. Diverse types of the sediment deposits filling the trench in its northern and southern part differ in substrate content: more volcanic sediments are in the south comparing to the northern part, which can be influenced by the different seismic settings and sediment transport paths. Steeper landforms are in general observed in the southern part of the trench comparing to those in its northern segment. In both southern and northern parts of the trench, the floor deposits are influenced by the lateral and longitudinal sediment supply.

The results of the comparative analysis of the two distinct parts of the trench located north- and southwards from the Bussol Strait show that southern part is deeper reaching -8,200 m depth while northern part has -7,800 at maximal records. The data analysis was performed to examine the spatial variation of the trench geomorphology including the interrelationships of the factors affecting its variation (geodetic, seismic, geologic and bathymetric).

Variations in the earthquakes magnitude and seismicity in the study area that are higher in the south-western part of the trench, as well as to a lesser extent location in the magnetic anomalies located in the north-east, influence the bathymetric patterns that show deeper values in the southern part and geomorphic landforms distribution. The cross-section profiles across the northern part of the KKT show deeper values of the depth and less steep slopes comparing to the southern segment, which refer to the erosional moats and drift of the submarine sediments.

On the contrary, southern profiles along the trench, comparing to the northern segment, located near the intense volcanic area demonstrate erosional moats at -3000 m depths adjusting the Greater Kuril Chain. This reflects a series of recent earthquakes erupted near Shikotan Island in the southern part of the Kuril-Kamchatka Trench. Besides, the anomalous metallogeny of the southern Kuril segment is determined by the deep geodynamics, which provided the impact of fluid energy fluxes from sub-subduction and supra-subduction asthenospheric zones. The profiles in the southern segment of the trench show more complex pattern of the processes of erosion along the upper slope and sediment deposition comparing to the northern segment. Therefore, the landward oriented submarine ridges of the trench facing the Greater Kuril Chain form oblique landform shape towards the coast of the southern Kurils. Southern part of the trench follows the exposition to the erosion processes in NE to SW direction caused by the intense earthquakes located on the south of the Greater Kuril Chain.

Northern part of the trench affected by numerous earthquakes located on the Kamchatka Peninsula (Figure 2) is influenced by the large amount of the accumulated sediments. Necessarily it forms the shallower depths and gentle flat slopes in the morphology of the northern part of the

KKT. On the contrary, the southern part is presented by V-shape formed slopes and steeper morphology which is affected by the specific geophysical conditions of the southern part of the Kuril Islands characterized by the magnetized anomaly zones of the oceanic crust. The junction of two different segments of the Kuril Islands, southern and northern, corresponds to a sub-latitudinal magnetic anomaly. The north-east direction of the magnetic anomalies are recorded on the oceanic slope of the trench up to its island slope while the southern segment of the trench axis is oriented in parallel.

The orthogonal bathymetric profiles across the southern and northern segments of the KKT identify two distinct U- and V-shaped morphologic features with affecting dominant processes: (1) in its northern segment, the dominant processes along the Kamchatka Peninsula are sediment deposition; (2) southern part located near the Hokkaido, Iturup and Urup islands and minor island of the Greater Kuril Chain are distinct by the processes of erosion and intense sediment transportation. The explosive volcanism in different parts of the KKT explain a high mass of sediments formed by gradual sediment accumulation.

The formation of the hadal trench is affected by the impacts of local geological, geophysical and oceanological settings that have resulted during the complex process of the tectonic plates movements and subduction. At the same time, there are local variations in northern and southern parts of the seafloor that influence the shape of the slopes. In the subduction zone of the Pacific plate, these cross-sections of the tilted trench illustrate the crustal processes of the subduction and deposition of deep-sea sediments into the trench in its both segments. The sediment dispersal system of the trench forms two distinct types: the first one is a trench-parallel and a second one is a trench-crossing system. The geological parameters visualized on the Figure 2 show fracture lines that predominantly have south-eastern direction showing perpendicular stretching towards the trench general direction.

The geomorphology of the KKT includes main submarine landforms related to the sedimentation processes, volcanic activities, tectonics, geologic formation history and regional oceanographic processes. The more important of them are as follows: 1) system of connected canyons and channels; 2) gullies, and deep-sea fans located on the slopes; 3) turbidity currents; 4) Drifts, moats and abyssal channels driven by the ocean circulations; 5) rotational deep-seated landslides triggered by the instability of the trench slopes and mass-transportation connected to the geologic underlying rocks structure; 6) craters associated with deep-sea fluid-flow processes.

Historically, the KKT subduction zone experienced a variety of large tsunamis along the trench (Zayakin and Luchinina, 1987). Reports on the seismicity of the KKT are provided by numerous studies (Kao and Chen, 1994; Gorbatov et al., 1997; Ruppert et al., 2007). The maximum depth of the seismicity along the KKT changes gradually from ca. 600 km to ca. 300 km with latitude increasing in a central part from ca. 50°N to ca. 54°N (Gorbatov et al., 2001), and then decreasing sharply to a depth of 100 km northwards. The rate occurrence of the tsunami on the Shikotan Island, the southern end of the Kuril Island Chain, is one per 250 yr. The most active section of the KKT subduction zone is the southern Kuril Islands and Hokkaido sections with nine Mw 7.5-8.5 earthquakes (NGDC/WDS, 2014, cited by: MacInnes et al., 2016). Larger earthquakes estimated as Mw 9.0 occur only every ca. 500 yr on Iturup Island (Iliev et al., 2005). Such seismic situation in the KKT makes this area in the north-west Pacific coast a tsunami-prone region (Gusiakov, 2016). The focal mechanism of the strongest earthquakes ( $M \geq 5$ ) in the southern part

of the KKT affects the orientation of the trench in this part through the main fracture zones with respect to the direction and type of the geomorphic displacements.

The formation of a variety of landforms including terraces and slopes of the trench reflects the complex action of a range of factors. These include tectonic, sedimentary, oceanographic, biochemical processes and hydrodynamic phenomena. As a result, the morphological character of the seabed in both southern and northern part is depending on the local and regional factors. The Greater Kuril Chain forms a natural barrier dividing the Sea of Okhotsk basin from the Pacific Ocean by the chain of islands and adjacent KKT, as well as separated into two parts by the Bussol Strait. The lateral slopes of the KKT are formed by the cumulative effects of the geologic, seismic and sedimentary factors at the subducting tectonic plate boundaries.

Technically, the comparison of the two parts of the trench was performed by means of the set of the cross-section profiles plotted by GMT in an automatic regime for northern and southern part of the trench. The morphology of both segments was then compared with aim to identify the characteristics of the trench geomorphology.

## Conclusion

The Kuril-Kamchatka subduction zone, a part of the circum-Pacific ‘Ring of Fire’, forms the northern part of the Kuril-Kamchatka volcanic arc in the North-West Pacific Ocean (Portnyagin and Manea, 2008; Gorshkov, 1958). The subduction rate of the Pacific plate beneath the Eurasian plate is  $\sim 79$  mm yr<sup>-1</sup> (DeMets et al., 1990; Bindeman et al., 2010) or 8–9 m per century along the KKT (Nanayama et al., 2003). This causes high seismic and volcanic activities, making this region one of the most tectonically active, seismic regions of the world. More specifically, one of the most active volcanic arcs in the world is located on the eastern coast of Kamchatka (Gorbatov et al., 2001; Pinegina et al., 2000). A number of studies analyzed earthquakes across the region of the southern Okhotsk Sea in the adjacent Kamchatka Peninsula. Nowadays, there are 29 active, and ca. 300 extinct volcanoes located on the Kamchatka Peninsula near the KKT (Solomina et al., 2007).

The KKT belongs to the Chilean tectonic subduction type, which has a gentle subduction dip advancing at a speed of ca. 2 cm yr<sup>-1</sup> and inter-seismic elastic shortening of 1–2 mm yr<sup>-1</sup> (DeMetz et al., 2010). Strong lateral velocity in the shallower mantle wedge accounts for both the compressional subduction tectonics and back arc compression in the KKT. This results in the seismic-velocity anomalies in the mantle under the KKT, as shown on the tomographic images by Yoshida (2017). Despite the age of the Pacific plate, there is no sharp variation of the age on the seafloor along the KKT (Renkin & Sclater, 1988), and the old Pacific Plate is rejuvenated at the north of the KKT around the Meiji Guyot seamount.

Southern part of the KKT differ, as proved by recent findings (Khomich et al., 2019) where it is demonstrated on the example of South Kuril that intense fluid thermal fluxes in the continental lithosphere cause of the formation of magmatic chambers and the development of volcanism and multi-metal ores. Over 700 earthquakes with hypo-centers >50 km are recorded in the KKT focal zone (Beck & Ruff, 1987). Individual earthquakes show large variations in seismic slip and distribution of foreshocks and aftershocks that shows spatial heterogeneity in the stress level and geological settings along the tectonic plate boundary (Ruff & Kanamori, 1983).



Northern part of the KKT located northwards from the Bussol strait presents a geographically complicated region with smaller islands than in other parts of the Kuril volcanic arc (MacInnes et al., 2016). This area is notable for the abnormally high heat flow in the ocean floor. Reduced thermal thickness of the Pacific Plate upon its subduction into the northern KKT indicates underlying mantle plume and point out that thermal thickness of the underlying plate is lesser than expected comparing to the normal oceanic plate of such age (Smirnov et al., 1992; Selivestrov, 1998; Smirnov & Sugrobov, 1980a; Smirnov & Sugrobov, 1980b).

### Acknowledgements

This research was funded by the China Scholarship Council (CSC), State Oceanic Administration (SOA) Marine Scholarship of China, Grant#2016SOA002, Beijing, China.

**Conflict of Interest:** The author declare that they have no conflict of interest.

**Ethical approval:** For this type of study formal consent is not required.

### References

- Barr, I. D., & Spagnolo, M. (2013). Palaeoglacial and palaeoclimatic conditions in the NW Pacific, as revealed by a morphometric analysis of cirques upon the Kamchatka Peninsula. *Geomorphology*, 192, 15-29.
- Brandt A., Alalykina, I., Fukumori, H., Golovand, O., Kniesz, K., Lavrenteva, A., Lörz, A.-N., Malyutina, M., Philipps-Bussau, K., & Stransky, B. (2018). First insights into macrofaunal composition from the SokhoBio expedition T (Sea of Okhotsk, Bussol Strait and northern slope of the Kuril-Kamchatka Trench). *Deep-Sea Research Part II*, 154, 106-120.
- Beck, S. L., & Ruff, L. J. (1987). Rupture process of the great 1963 Kurile Islands earthquake sequence: asperity interaction and multiple event rupture. *Journal of Geophysical Research*, 92(14), 123-138.
- Bindeman, I. N., Leonov, V. L., Izbekov, P. E., Ponomareva, V. V., Watts, K. E., Shipley, N., Perepelov, A. B., Bazanova, L. I., Jicha, B. R., Singer, B. S., Schmitt, A. K., Portnyagin, M. V., & Chen, C. H. (2010). Large-volume silicic volcanism in Kamchatka: Ar–Ar and U–Pb ages, isotopic, and geochemical characteristics of major pre-Holocene caldera-forming eruptions. *Journal of Volcanology and Geothermal Research*, 189(1), 57–80.
- DeMets, C., Gordon, R. G., & Argus, D. F. (2010). Geologically current plate motions. 2010. *Geophysical Journal International*, 181, 1-80.
- DeMets, C., Gordon, R. G., Argus, D. F., & Stein, S. (1990). Current plate motions. *Geophysical Journal International*, 101(2), 425–478.
- Dobrovolski, A. D. & Zalogin, B.S. (1982). *Seas of USSR*. Moscow: Moscow University Press. [in Russian].
- Gauger, S., Kuhn, G., Gohl, K., Feigl, T., Lemenkova, P., Hillenbrand, C. (2007). Swath-bathymetric mapping. Reports on Polar and Marine Research, 557, 38–45.

- Gorbatov, A., Fukao, Y., Widiyantoro, S. & Gordeev, E. (2001). Seismic evidence for a mantle plume oceanwards of the Kamchatka–Aleutian trench junction. *Geophysical Journal International*, 146, 282-288.
- Gorbatov, A., Kostoglodov, V., Suarez, G., & Gordeev, E. (1997). Seismicity and structure of the Kamchatka subduction zone, *Geophysical Journal International*, 102(17), 883-898.
- Gorshkov, G. S. (1958). *Catalog of the Active Volcanoes of the World Including Solfatara Fields*. P. VII. Kurile Islands. Napoli: International Volcanological Association Press.
- Gusiakov, V. K. (2016). Tsunamis on the Russian Pacific coast: history and current situation. *Russian Geology and Geophysics*, 57, 1259-1268.
- Iliev, A. Y., Kaistrenko, V. M., Gretskeya, E. V., Tikhonchuk, E. A., Razjigaeva, N. G., Grebennikova, T. A., Ganzey, L. A., & Kharlamov, A. A. (2005). *Holocene tsunami traces on Kunashir Island, Kurile subduction zone*, in: Satake, K. (Ed.), *Tsunamis: Case Studies and Recent Developments*. Advances in Natural and Technological Hazards Research. Netherlands: Springer, 171-192.
- Kao, H., & Chen, W. (1994). The double seismic zone in Kuril-Kamchatka: the tale of two overlapping single zones. *Geophysical Journal International*, 99 (B4), 6913-6930.
- Kasahara, J., Sato, T., Mochizuki, K. & Kobayashi, K. (1997). Paleotectonic structures and their influence on recent seismo-tectonics in the south Kuril subduction zone. *Island Arc*, 6, 267–280.
- Khomich, V. G., Boriskina, N. G., & Kasatkin, S. A. (2019). Geology, magmatism, metallogeny, and geodynamics of the South Kuril Islands. *Ore Geology Reviews*, 105, 151-162.
- Klaučo, M., Gregorová, B., Stankov, U., Marković, V., & Lemenkova, P. (2013). Determination of ecological significance based on geostatistical assessment: a case study from the Slovak Natura 2000 protected area. *Central European Journal of Geosciences* 5(1), 28–42.
- Klaučo, M., Gregorová, B., Stankov, U., Marković, V., Lemenkova, P. (2014). Landscape metrics as indicator for ecological significance: assessment of Sitno Natura 2000 sites, Slovakia. Ecology and Environmental Protection. Proceedings of the Int'l Conference, Minsk, Belarus: BSU Press, 85–90.
- Klaučo, M., Gregorová, B., Stankov, U., Marković, V., Lemenkova, P. (2017). Land planning as a support for sustainable development based on tourism: A case study of Slovak Rural Region. *Environmental Engineering and Management Journal*, 2(16), 449-458.
- Kuhn, G., Hass, C., Kober, M., Petitat, M., Feigl, T., Hillenbrand, C. D., Kruger, S., Forwick, M., Gauger, S., Lemenkova, P. (2006). The response of quaternary climatic cycles in the South-East Pacific: development of the opal belt and dynamics behavior of the West Antarctic ice sheet. *Expeditionsprogramm Nr. 75 ANT XXIII/4*, AWI, Germany.
- Lemenkova, P. (2011). *Seagrass Mapping and Monitoring Along the Coasts of Crete, Greece*. M.Sc. Thesis. Netherlands: University of Twente, 158 pp.

- Lemenkova, P., Promper, C., Glade, T. (2012). Economic Assessment of Landslide Risk for the Waidhofen a.d. Ybbs Region, Alpine Foreland, Lower Austria. Protecting Society through Improved Understanding. 11th Int'l Symposium on Landslides & the 2nd North American Symposium on Landslides & Engineered Slopes (NASL), Banff, Canada, 279–285.
- Lemenkova, P. (2018a). R scripting libraries for comparative analysis of the correlation methods to identify factors affecting Mariana Trench formation. *Journal of Marine Technology and Environment*, 2, 35-42.
- Lemenkova, P. (2018b). Factor Analysis by R Programming to Assess Variability Among Environmental Determinants of the Mariana Trench, *Turkish Journal of Maritime and Marine Sciences*, 4, 146–155.
- Lemenkova, P. (2019a). An Empirical Study of R Applications for Data Analysis in Marine Geology. *Marine Science and Technology Bulletin*, 8(1), 1-9.
- Lemenkova, P. (2019b). Processing oceanographic data by Python libraries NumPy, SciPy and Pandas, *Aquatic Research*, 2, 73-91.
- Lemenkova, P. (2019c). Testing Linear Regressions by StatsModel Library of Python for Oceanological Data Interpretation, *Aquatic Sciences and Engineering*, 34, 51–60.
- Lemenkova, P. (2019d) Regression Models by Gretl and R Statistical Packages for Data Analysis in Marine Geology. *International Journal of Environmental Trends* 3(1), 39–59.
- Lemenkova, P. (2019e). Numerical Data Modelling and Classification in Marine Geology by the SPSS Statistics. *International Journal of Engineering Technologies*, 5(2), 90–99.
- Lemenkova, P. (2019f). AWK and GNU Octave Programming Languages Integrated with Generic Mapping Tools for Geomorphological Analysis. *GeoScience Engineering* 65(4), 1-22.
- Lemenkova, P. (2019g). Topographic surface modelling using raster grid datasets by GMT: example of the Kuril-Kamchatka Trench, Pacific Ocean. *Reports on Geodesy and Geoinformatics* 108, 9–22.
- Lemenkova, P. (2019h). GMT Based Comparative Analysis and Geomorphological Mapping of the Kermadec and Tonga Trenches, Southwest Pacific Ocean. *Geographia Technica* 14, 39–48.
- Lemenkova, P. (2019i). Plotting Ternary Diagrams by R Library ggtern for Geological Modelling. *Eastern Anatolian Journal of Science* 5 (2), 16–25.
- Lemenkova, P. (2019j). K-means Clustering in R Libraries {cluster} and {factoextra} for Grouping Oceanographic Data. *International Journal of Informatics and Applied Mathematics*, 2(1), 1–26.
- MacInnes, B., Kravchunovskaya, E., Pinegina, T., & Bourgeois, J. (2016). Paleotsunamis from the central Kuril Islands segment of the Japan-Kuril-Kamchatka subduction zone. *Quaternary Research*, 86, 54-66.

- Maiorova, A. S. & Adrianov, A.V. (2018). Deep-sea sipunculans from the Kuril Basin of the Sea of Okhotsk and the T adjacent slope of the Kuril-Kamchatka Trench. *Deep-Sea Research Part II*, 154, 167–176.
- Nanayama, F., Satake, K., Furukawa, R., Shimokawa, K., Atwater, B. F., Shigeno, K., & Yamaki, S. (2003). Unusually large earthquakes inferred from tsunami deposits along the Kuril trench. *Nature*, 424 (6949), 660-663.
- NGDC/WDS (National Geophysical Data Center/World Data Service). *Global Historical Tsunami Database*. National Geophysical Data Center, NOAA.
- Pflanz, D., Gaedicke, C., Freitag, R., Krbetschek, M., Tsukanov, N., & Baranov, B. (2013). Neotectonics and recent uplift at Kamchatka and Aleutian arc junction, Kamchatka Cape area, NE Russia. *International Journal of Earth Sciences*, 102, 903–916.
- Pinegina, T. K., Bourgeois, J., Kravchunovskaya, E. A., Lander, A. V., Arcos, M. E., Pedoja, K., & MacInnes, B. T. (2013). A nexus of plate interaction: vertical deformation of Holocene wave-built terraces on the Kamchatsky Peninsula (Kamchatka, Russia). *Geological Society of America Bulletin*, 125 (9-10), 1554–1568.
- Portnyagin, M., Manea, V. C. (2008). Mantle temperature control on composition of arc magmas along the Central Kamchatka Depression. *Geology*, 36, 519-522.
- Renkin, M. L., Sclater, J. G. (1988). Depth and age in the North Pacific, *Journal of Geophysical Research*, 93, 2919–2935.
- Ruff, L., Kanamori, H. (1983). The rupture process and asperity distribution of three great earthquakes from long-period diffracted P-waves. *Physics of the Earth and Planetary Interiors*, 31, 202-230.
- Ruppert, N. A., Lees, J. M., & Kozyreva, N. P. (2007). Seismicity, earthquakes and structure along the Alaska-Aleutian and Kamchatka-Kurile Subduction Zones: a review. *Geophysical Monograph Series*, 172 doi:10.1029/172GM12
- Schenke, H. W., Lemenkova, P. (2008). Zur Frage der Meeresboden-Kartographie: Die Nutzung von AutoTrace Digitizer für die Vektorisierung der Bathymetrischen Daten in der Petschora-See. *Hydrographische Nachrichten*, 25(81), 16–21.
- Selivestrov, N. I. (1998). *Structure of the oceanic floor near Kamchatka and the geodynamics of the zone of Kuril-Kamchatka and Aleutians trenches Joint*. Moscow: Nauchni Mir [in Russian].
- Smirnov, Y. B., Sugrobov, V. M. & Yanovskiy, F. A. (1992). The terrestrial heat flow of Kamchatka, *Journal of Volcanology and Seismology*, 13, 181–210.
- Smirnov, Y. B., & Sugrobov, V. M. (1980a). Terrestrial heat flow in the Kurile-Kamchatka & Aleutian provinces—II, The map of measured and background heat flow, *Journal of Volcanology and Seismology*, 1, 16-31 [in Russian].



- Smirnov, Y. B., & Sugrobov, V. M. (1980b). Terrestrial heat flow in the Kurile-Kamchatka and Aleutian provinces—III, Assessment of temperature at depth and thickness of the lithosphere, *Journal of Volcanology and Seismology*, 2, 3-18 [in Russian].
- Smith, W. H. F., & Sandwell, D. T. (1997). Global seafloor topography from satellite altimetry and ship depth soundings. *Science*, 277, 1957-1962.
- Solomina, O., Wiles, G., Shiraiwa, T., & D'Arrigo, R. (2007). Multiproxy records of climate variability for Kamchatka for the past 400 years. *Climate of the Past* 3 (1), 119-128.
- Suetova, I., Ushakova, L., Lemenkova, P. (2005). Geoinformation mapping of the Barents and Pechora Seas. *Geography and Natural Resources* 4, 138–142.
- Wessel, P., & Smith, W. H. F. (1991). Free software helps map and display data. *EOS Transactions of the American Geophysical Union*, 72, 441.
- Wessel, P., & Smith, W. H. F. (1996). A Global Self-consistent, Hierarchical, High-resolution Shoreline Database. *Journal of Geophysical Research*, 101, 8741–8743.
- Wessel, P., & Smith, W. H. F. (1998). New version, of the Generic Mapping Tools re- leased. *EOS Transactions of the American Geophysical Union*, 79(47), 329. doi: 10.1029/98EO00426
- Wessel, P., & Smith, W. H. F. (2018). *The Generic Mapping Tools. Version 4.5.18 Technical Reference and Cookbook* [Computer software manual]. U.S.A.
- Wessel, P., Smith, W. H. F., Scharroo, R., Luis, J., & Wobbe, F. (2019). *The Generic Mapping Tools. GMT Man Pages. Release 5.4.5* [Computer software manual]. U.S.A.
- Yoshida, M. (2017). Trench dynamics: Effects of dynamically migrating trench on subducting slab morphology and characteristics of subduction zones systems. *Physics of the Earth and Planetary Interiors*, 268, 35–53.
- Zayakin, Y. A., & Luchinina, A. A. (1987). *Catalogue of Tsunamis on Kamchatka*. Obninsk: VNIIGMI-Mtsd. [in Russian].